

SCIENTIFIC REPORTS



OPEN

Membrane damage mechanism contributes to inhibition of trans-cinnamaldehyde on *Penicillium italicum* using Surface-Enhanced Raman Spectroscopy (SERS)

Fei Huang^{1,2,3}, Jie Kong^{1,2,3}, Jian Ju^{1,2,3}, Ying Zhang^{1,2,3}, Yahui Guo^{1,2,3}, Yuliang Cheng^{1,2,3}, He Qian^{1,2,3}, Yunfei Xie^{1,2,3} & Weirong Yao^{1,2,3}

The antifungal mechanism of essential oils against fungi remains in the shallow study. In this paper, antifungal mechanism of trans-cinnamaldehyde against *Penicillium italicum* was explored. Trans-cinnamaldehyde exhibited strong mycelial growth inhibition against *Penicillium italicum*, with minimum inhibitory concentration of 0.313 $\mu\text{g/mL}$. Conventional analytical tests showed that trans-cinnamaldehyde changed the cell membrane permeability, which led to the leakage of some materials. Meanwhile, the membrane integrity and cell wall integrity also changed. Surface-enhanced Raman spectroscopy, an ultrasensitive and fingerprint method, was served as a brand-new method to study the antifungal mechanism. Characteristic peaks of supernatant obviously changed at 734, 1244, 1330, 1338 and 1466 cm^{-1} . The Raman intensity represented a strong correlation with results from conventional methods, which made SERS an alternative to study antifungal process. All evidences implied that trans-cinnamaldehyde exerts its antifungal capacity against *Penicillium italicum* via membrane damage mechanism.

China is a large producer of citrus fruits¹, quantities of citrus fruits are stored for a long time for sale. Blue mold caused by *Penicillium italicum* (*P. italicum*) is one of the main diseases of citrus fruits during storage². Postharvest decay leads to tremendous economic losses³. In-depth study of the inhibitory mechanism of fungistat against *P. italicum* will help to develop more efficient and more reasonable new fungistat.

The development of isolates resistant to traditional synthetic chemicals involved in human health and environmental pollution has urged scientists to find new approaches to control the pathogens. Essential oils are new perspective to control citrus postharvest spoilage fungi, eliciting low toxic effects on mammals and strong inhibitory effects on food- or crop-contaminating fungi, such as *P. digitatum* and *P. italicum*⁴. Trans-cinnamaldehyde, main component of cinnamon oil and a safe food additive widely used in food industry⁵, exerts an excellent growth inhibition of bacteria and fungi^{6,7}. However, antifungal mechanism of essential oils against fungi remains in shallow study, and molecular level research was rarely reported. Traditional characterization methods do not provide fingerprint analysis at molecular level.

Raman spectroscopy is a vibrational spectroscopic method that provides the fingerprint characteristics on various chemical and biochemical components in a complex system^{8,9}. But Raman signal is relatively weak¹⁰, which limited its applications. Surface-enhanced Raman spectroscopy possesses extremely high sensitivity and provide fingerprint information of various molecules with the strong electromagnetic enhancement typically provided by Ag or Au NPs, the enhancement reaches 10^3 – 10^6 fold compared with the normal Raman scattering process¹¹, which makes SERS an ultrasensitive detection tool, even down to single molecule level¹². Thus, the changes in cellular composition such as in lipids, proteins, and nucleic acids can be monitored by SERS¹³. Due to

¹State Key Laboratory of Food Science and Technology, Jiangnan University, Jiangsu Province, China. ²School of Food Science and Technology, Jiangnan University, Jiangsu Province, China. ³Joint International Research Laboratory of Food Safety, Jiangnan University, No. 1800 Lihu Avenue, Wuxi, 214122, Jiangsu Province, China. Correspondence and requests for materials should be addressed to Y.X. (email: xieyunfei@jiangnan.edu.cn)

its advantages, many researches were conducted with SERS to study the antibacterial activity and mechanism of drugs^{14–16} or particles^{13,17}. However, utilize of SERS to research the antifungal activity and mechanism of essential oils was rarely reported. Only few literature had recorded the brilliant study of antifungal mechanism using SERS, nevertheless, they were just limited to studying yeast^{18–20}. Thus, SERS seems to be a new and potential alternative for antifungal mechanism studying.

In this research, antifungal mechanism of trans-cinnamaldehyde on *P. italicum* was going to be studied with the traditional methods, such as antifungal assay, test of permeability of cell membrane, and determination of integrity of plasma membrane and so on. Sequentially, SERS was planned to be developed as a new alternative to analyze the antifungal mechanism. After preparing colloidal Au nanoparticles, the supernatant of trans-cinnamaldehyde treated mycelium suspension would be detected using SERS. Some typical strong peaks was likely to be assigned to nucleic acid, protein and lipid. The correlation between Raman intensities and the results obtained from traditional methods could be analyzed. This report promise the potential application of SERS in interpretation of the antifungal process in future.

Material and Methods

Chemicals and pathogen. Trans-cinnamaldehyde ($\geq 95\%$) was purchased from Shanghai Shuangxiang auxiliaries plant (Shanghai, China). Propidium iodide ($\geq 95\%$), Bovine serum albumin ($\geq 96\%$), potassium auric chloride (original Au $\geq 99.95\%$), and sodium citrate (99%) were bought from Nanjing Senbeijia biological technology Co., Ltd (Nanjing, China). Coomassie brilliant blue G-250 (90%) was obtained from Sinopharm chemical reagent Co., Ltd (Shanghai, China). All the chemicals were analytic grade. The water, except special statement, was deionized water.

P. italicum was obtained from China General Microbiological Culture Collection Center (CGMCC) (Beijing, China). All the test strains were preserved on potato dextrose agar (PDA) at $28 \pm 2^\circ\text{C}$. Conidial spore concentration was adjusted to 1×10^6 cfu/mL with Haemocytometer.

Antifungal assay. Several essential oils were tested to assess their capacity of inhibitory effect against *P. italicum*. The experiment was demonstrated using Microtitre Plate Well Assay²¹. 100 μL sterilized potato dextrose broth (PDB) was injected into 96-well plates. 100 μL essential oils diluted in ethanol was injected into the first well, 2 fold diluted. Then, 100 μL conidial spore suspension (1×10^6 cfu/mL) was poured into each well. Finally, the 96-well plate was incubated at $28 \pm 2^\circ\text{C}$ in the constant temperature incubator for 48 h. The lowest concentration that completely inhibited the growth of the fungus was considered the minimum inhibitory concentration (MIC).

The mycelial growth inhibition was carried out following previous work²². Different amounts of trans-cinnamaldehyde were added to 50 mL PDB liquid medium with the final concentration of trans-cinnamaldehyde 0.000, 0.020, 0.040, 0.078, 0.156, 0.313 0.625 $\mu\text{L}/\text{mL}$. Then, 200 μL conidial spore suspension was inoculated in each triangle bottle, which was incubated at $28 \pm 2^\circ\text{C}$ in a rotatory shaker at 120 r/min for 2 d. Fungal growth inhibition was estimated gravimetrically by weighting the biomasses after drying at 80°C to a constant weight. The percentage of mycelial growth inhibition (PGI) was calculated according to the following formula:

$$\text{PGI}(\%) = \left[\frac{wc - wt}{wc} \right] \times 100$$

where wc (g) is net dry weight of control fungi and wt (g) is net dry weight of treated fungi.

Test of plasma membrane integrity. At the beginning, aliquot of 1 mL conidial spore suspension was transferred into 50 mL triangle bottles with 10 mL PDB to obtain a final concentration of 1×10^6 cfu/mL, incubated at $28 \pm 2^\circ\text{C}$ in a rotatory shaker at 120 r/min for 7 h. Different amounts of trans-cinnamaldehyde were added to triangle bottles. PDB without trans-cinnamaldehyde served as control. To assay the effect of trans-cinnamaldehyde on plasma membrane integrity, conidial spores of *P. italicum* were collected from PDB medium at 0, 2, 4 and 6 h.

Membrane integrity was assayed following reported work²³ with some modifications. The time of collecting conidial spores was described above. Spores in PDB were collected by centrifugation at $10000 \times g$ for 3 min at room temperature, and washed twice with 0.2 mol/L sodium phosphate buffer (pH 7.0) to remove residual medium. The conidial spores were stained with 10 $\mu\text{g}/\text{mL}$ propidium iodide (PI) for 5 min at 30°C . Spores were then collected by centrifugation, washed twice with the sodium phosphate buffer (pH 7.0) to remove residual dye. The spores were observed with Inverted Fluorescence Microscope (Carl Zeiss Vision, Germany) equipped with an individual fluorescein rhodamine filter set (Zeiss no. 15: excitation BP 546/12 nm, LP590 nm). Five fields of view from each cover slip were chosen randomly, and the number of spores in bright-field was defined as the total number. Membrane integrity (MI) was calculated according to the formula:

$$\text{MI}(\%) = \frac{\text{No. of total spores} - \text{No. of stained spores}}{\text{No. of total spores}} \times 100$$

Measurement of reactive oxygen species. Determination of accumulation of reactive oxygen species (ROS) was carried out by reference to luminol chemiluminescence. Two-day-old mycelium from PDB collected by vacuum filtration was grounded into powder with liquid nitrogen. The supernatant from centrifuge was put on ice waiting for next step. 50 μL supernatant and 830 μL HEPES buffer (0.02 mol/L, pH 7.4) were injected into a glass container. Start MPI-B Chemiluminescence analysis test system (Xi'an Ruimai Analytical Instrument

Name of essential oils	Minimum inhibitory concentration
Salicylic acid	2.590 mg/mL
Cinnamic acid	0.400 mg/mL
Thymol	15.938 mg/mL
Carvacrol	0.625 μ g/mL
Eugenol	2.500 μ g/mL
Carvone	0.750 μ g/mL
Trans-Cinnamaldehyde	0.313 μ g/mL
Citral	1.250 μ g/mL
Geraniol	3.750 μ g/mL
Hexanal	10.000 μ g/mL

Table 1. Minimum inhibitory concentration of various essential oils against *P. italicum*.

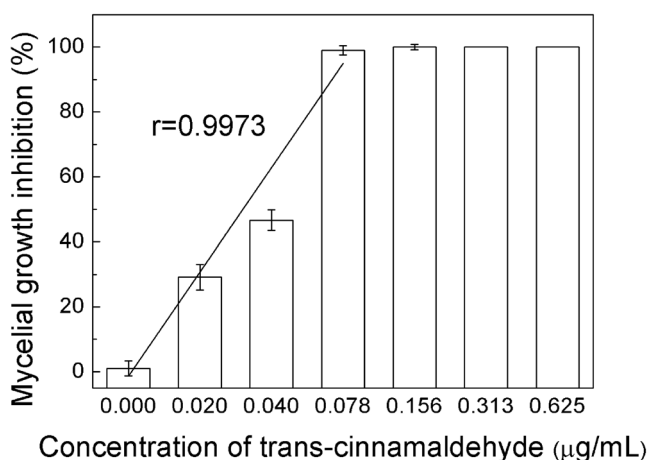


Figure 1. Mycelial growth inhibition of *P. italicum* under different concentration of trans-cinnamaldehyde.

Co., Ltd., China) immediately when 20 μ L horseradish peroxidase (3 mg/mL) was added under absolutely dark environment.

Measurement of intracellular constituents leakage. *Measurement of soluble protein leakage.* Measurement of intracellular soluble protein leakage was accorded to the method reported previously²⁴ with modifications. An aliquot of 200 μ L conidial spore suspension (1×10^6 cfu/mL) was transferred to triangle bottles with 100 mL PDB, cultured at $28 \pm 2^\circ\text{C}$ in a rotatory shaker at 120 r/min for 2 d. Mycelium was collected by vacuum filtration, washed twice with sterilized distilled water. About 1 g fresh mycelium was resuspended in 30 ml 0.85% saline, into which trans-cinnamaldehyde was poured and adjusted to 0, 0.5, 1, 2 MIC. The bottles were inoculated at $28 \pm 2^\circ\text{C}$ in a rotatory shaker at 120 r/min. 2 mL of the suspension was collected at 0, 30, 60, 120 min, and centrifuged at $10000 \times g$, 5 min. 1 mL of supernatant was transferred into Eppendorf tube and 5 mL of 0.1 mg/mL Coomassie brilliant blue G-250 followed. After 10 min inoculated at room temperature, absorbance at 595 nm was measured. Bovine Serum Albumin (BSA) served as standard. The results were expressed as μ g of soluble protein per g of fresh mycelium. The experiment was conducted three times.

Measurement of release of constituents absorbing at 260 nm. The release of constituents absorbing at 260 nm was measured referring to reported method²⁵ with minor modifications. About 1 g fresh mycelium was resuspended in 50 mL 0.85% saline, into which trans-cinnamaldehyde was poured and adjusted to 0, 0.5, 1, 2 MIC. The bottles were inoculated at $28 \pm 2^\circ\text{C}$ in a rotatory shaker at 120 r/min. 2 mL of the suspension was collected at 0, 30, 60, 120 min, and centrifuged at $10000 \times g$, 5 min. 1 mL of supernatant was used to determine the constituents absorbing at 260 nm by absorbance at 260 nm.

Determination of potassium ions efflux. A previously reported method was used to determine the amount of potassium ions efflux²⁶ with modifications. Detailedly, two-day-old mycelium cultured in PDB was collected by vacuum filtration. The concentration of free potassium ions in suspension was determined after the exposure to trans-cinnamaldehyde at 0, 0.5, 1, 2 MIC in ultrapure water for 0, 30, 60, 120 min. At each pre-established interval, free potassium ions in the supernatant was measured by a photometric procedure using

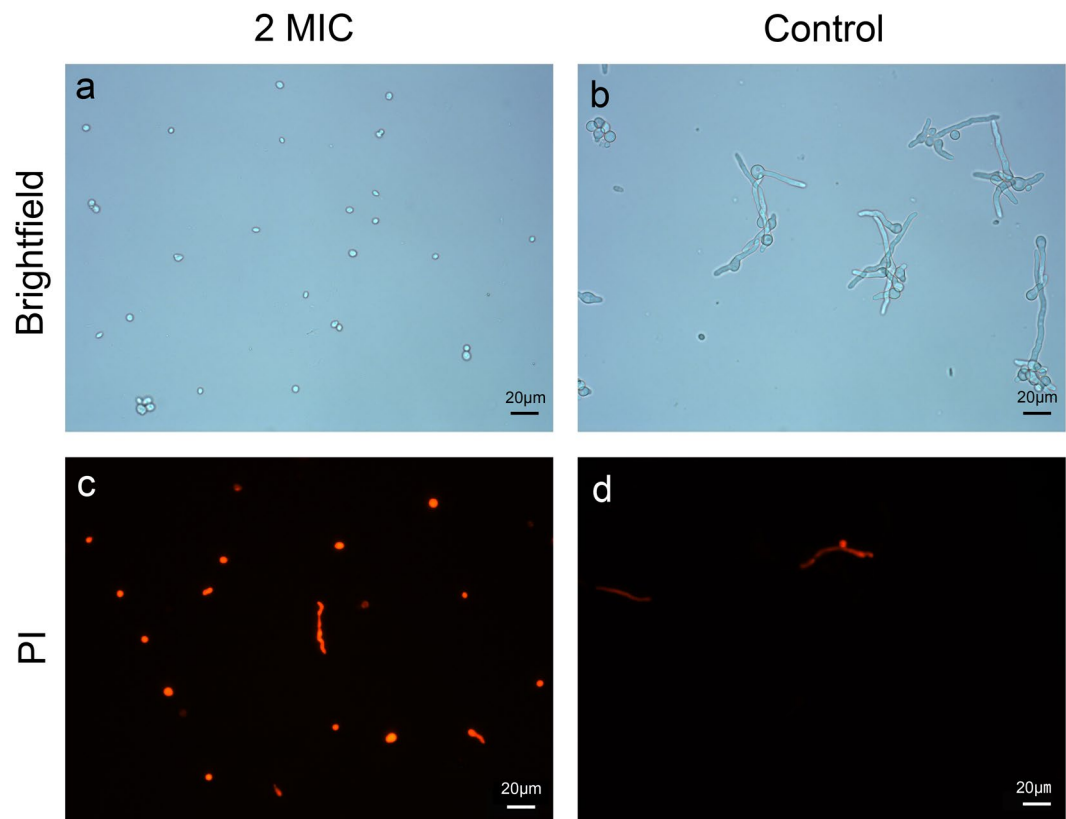


Figure 2. Optical microscope images of *P. italicum* spores after 6h treatment with 2 MIC trans-cinnamaldehyde.

the flame atomic absorption spectroscopy (Varian, USA). Results were expressed as amount of extracellular free potassium (mg/L) in the growth medium in each interval of incubation.

SEM of mycelium structure after treatment. Mycelium during logarithmic phase was pre-fixed with 5% glutaraldehyde in 0.1 mol/L phosphate buffer, pH 7.2, and rinsed with 0.1 mol/L phosphate buffer. Then the mycelium was pro-fixed with 1% tannic acid in 0.1 mol/L phosphate buffer, pH 7.2, and rinsed with 0.1 mol/L phosphate buffer, following which they were dehydrated in an ethanol series (30%, 50%, 70%, and 90%, v/v). After drying at the critical point in liquid carbon dioxide, the sample was attached to a sample stage. The specimen were coated with gold in an BAL-TEC, SCD 005 ion sputter (Hitachi, Japan), and then a FEI-Quanta 200 scanning electron microscope (Hitachi, Japan) was used to observe the sample, operating at 10kV at 1200x level of magnification.

Preparation of colloidal Au nanoparticles for SERS. 6 mL 1% potassium auric chloride was added to the round-bottom flask, 94 mL ultrapure water followed. The round-bottom flask was heated in oil bath at 120 °C. After ebullition, 4 mL sodium citrate was poured into the system. After maintaining ebullition for 30 min, the colloidal Au nanoparticles was prepared, and preserved in a brown bottle. All the containers were immersed in aqua regia overnight to wash impurities away.

SERS measurement of extracellular material. About 1 g two-day-old mycelium was collected with vacuum filtration and resuspended in 50 mL triangle bottle containing 20 mL 0.85% saline where trans-cinnamaldehyde was at 0, 0.5, 1, 2 MIC, respectively. 1 mL suspension was transferred to Eppendorf tube and centrifuged at 10000 × g, 5 min. 100 µL supernatant was drop in a glass cup (0.5 cm diameter) containing 400 µL colloidal Au nanoparticles, and mixed them thoroughly, then SERS was tested by the Raman spectrometer (OptoTrace Technologies, Inc. California, USA) with a fiber-optic probe and a CCD array detector. The emitted wavelength was 785 nm and the output power was 285 mW. Tree or more spectrum were gathered from one sample on different spots in order to ensure the reproducibility of SERS features.

Statistical analysis. All tests were conducted in triplicate, and all parameters were expressed as mean ± SD. Analysis of variance using one-way ANOVA followed by Duncan's test was performed to test the significance of differences between means obtained among the treatments at the 5% level of significance using SPSS statistical software package release 22.0 (SPSS Inc., Chicago, IL, USA). The SERS spectrum data were processed by origin-Pro 8.0 (OriginLab Corporation, USA), and the trend of Raman intensity elaborated in figures were expressed as the intensity of every peak using the baseline and peak function of OriginPro 8.0 (OriginLab Corporation, USA).

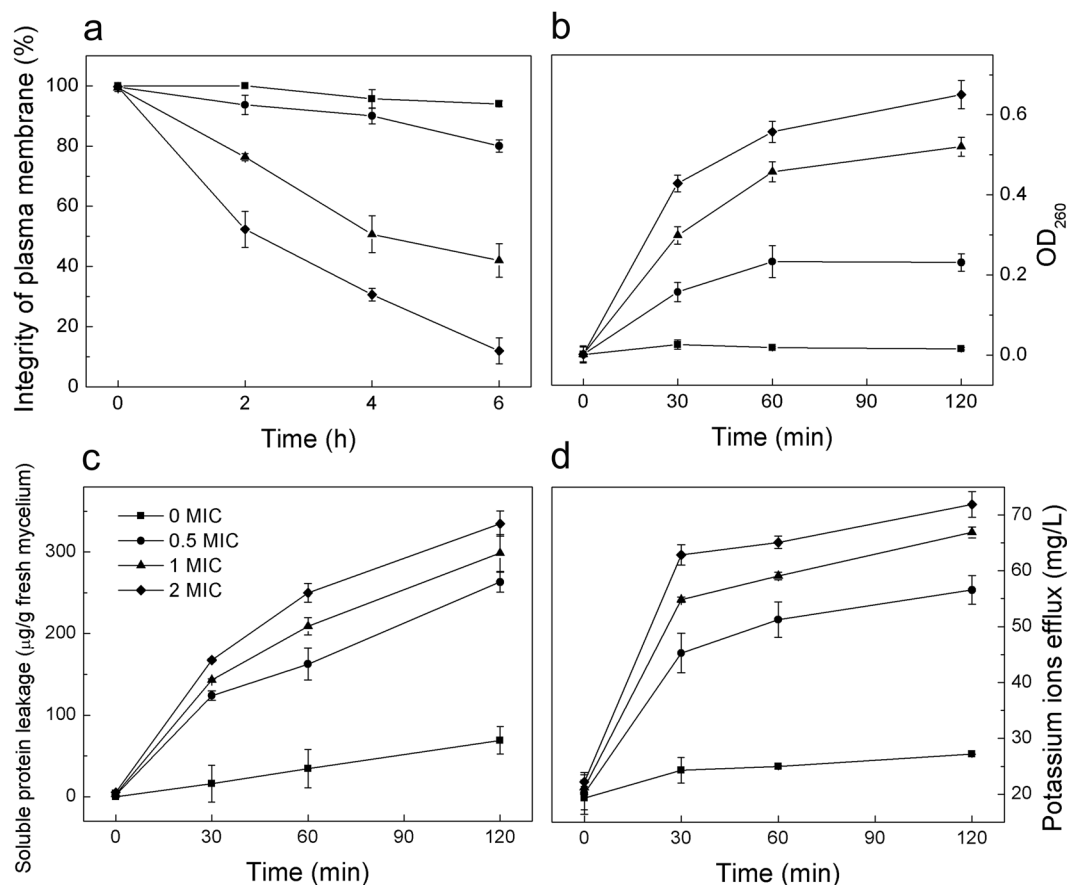


Figure 3. Tendency chart of some index. (a) plasma membrane integrity of *P. italicum* spores. (b) OD₂₆₀ value of constituents absorbing at 260 nm. (c) Soluble protein leakage. (d) Potassium ions efflux.

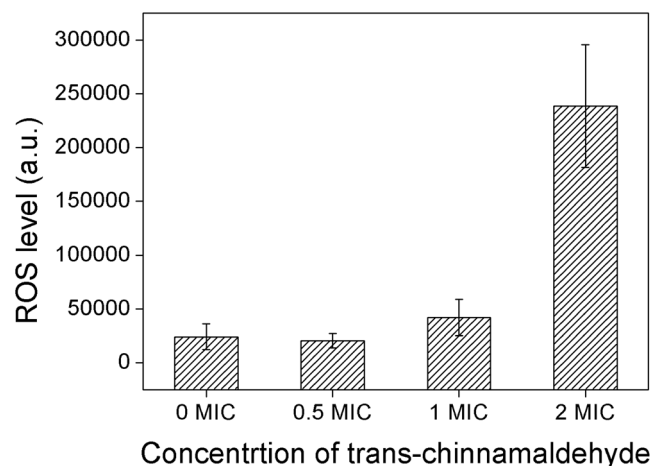


Figure 4. Level of ROS accumulating in mycelium after treating with different concentration of trans-cinnamaldehyde.

Results and Discussion

Inhibitory effect of trans-cinnamaldehyde on mycelial growth.

Microtitre Plate Well Assay proved that the lowest concentration of trans-cinnamaldehyde that completely inhibited the growth of the fungus was 0.313 μg/mL which was lower than that of other essential oils, showing in Table 1. Thus, the minimum inhibitory concentration (MIC) of trans-cinnamaldehyde was 0.313 μg/mL. The mycelial growth of *P. italicum* was strongly inhibited by trans-cinnamaldehyde in a dose-dependent manner ($r = 0.9973$) as shown in Fig. 1. Why the phenomenon that the mycelium growth had been inhibited nearly to 100% under 0.078 μg/mL concentration of

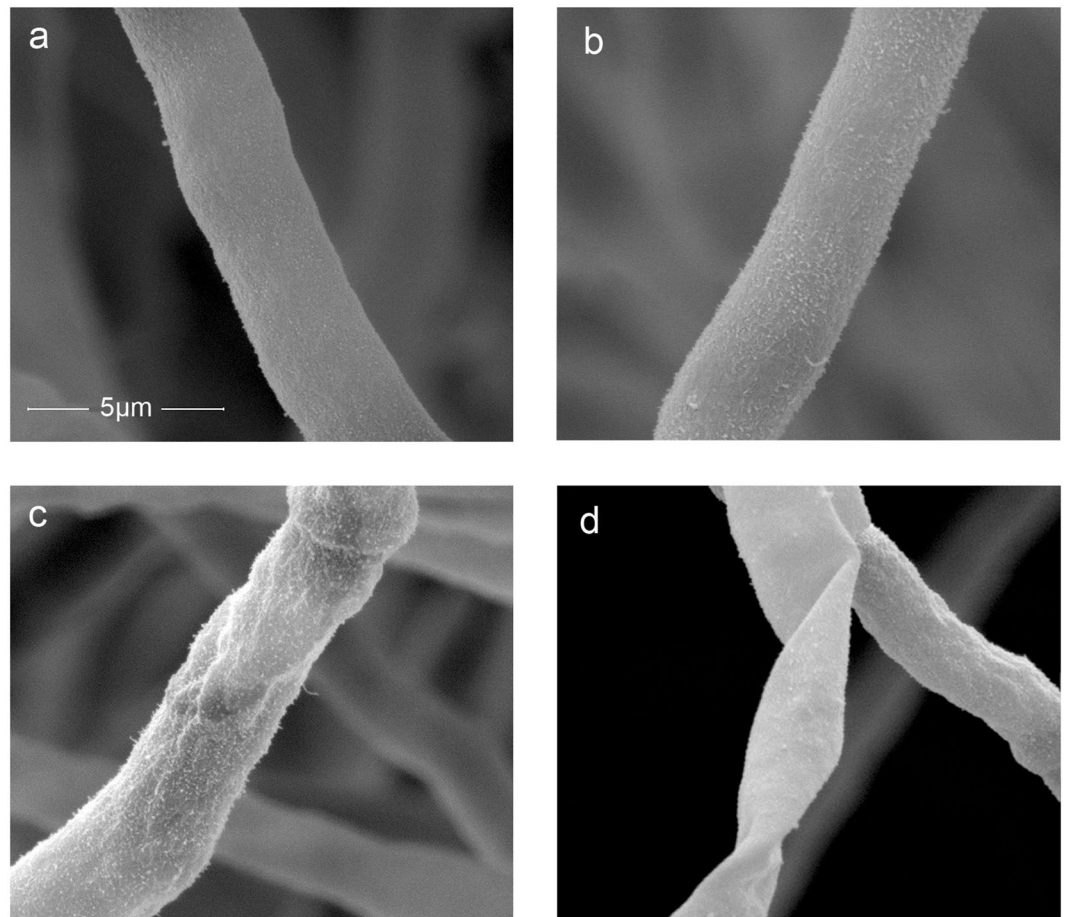


Figure 5. SEM images of mycelium treated under different concentrations. (a) control group. (b) 0.5 MIC treated group. (c) 1 MIC treated group. (d) 2 MIC treated group.

trans-cinnamaldehyde which was lower than MIC occurred is that different rate of spore suspension and PDB culture, which was determined by the method system and cannot be avoidable. Low magnitude of MIC made trans-cinnamaldehyde an excellent fungistat.

Effect of trans-cinnamaldehyde on plasma membrane integrity of *P. italicum* spores. To test the effect of trans-cinnamaldehyde on plasma membrane integrity, cells were dyed with propidium iodide. And results were shown in Fig. 2. The conidial spores had almost been stained after 6 h treatment with 2MIC trans-cinnamaldehyde, as shown in Fig. 2c. However, when contrasted the cells in bright field and dark field (Fig. 2b,d), it was found that nearly no cells were stained in control group. When observing the cells in bright field (Fig. 2a,b), it was easy to discover that the conidial spore germination had been inhibited to a great extent, which was corresponding to the antifungal assays.

MI of *P. italicum* spores under different dose of trans-cinnamaldehyde were elaborated in Fig. 3. According to Fig. 3a, MI of 2 MIC-treated *P. italicum* was 12% while that of control group was 94% after 6 h incubation. MI of *P. italicum* spores declined with the increase of incubation time in PDB containing different amount trans-cinnamaldehyde. Plasma membrane of *P. italicum* was obviously damaged in PDB with high level trans-cinnamaldehyde. Inversely, MI stayed at high level in control group without trans-cinnamaldehyde, indicating plasma membrane integrity remained complete. The action mode by which trans-cinnamaldehyde interfere the plasma membrane may be related to its dissolution into the hydrophobic domain of the cytoplasm membrane, between the lipid acyl chains, disintegrated the outer membrane of *P. italicum* and finally leading to cell death²⁷.

Release of constituents absorbing at 260 nm and soluble protein. Intracellular materials including nucleic acid which were absorbed at 260 nm in the suspensions as well as soluble protein plays an important role in cell live. Optical density at 260 nm (OD_{260}) were used to evaluate the leakage of nucleic acid. The release of constituents absorbing at 260 nm after *P. italicum* was treated with trans-cinnamaldehyde were shown in Fig. 3b. The value of OD_{260} in test group at 30 min were significantly different from what at 0 min ($P < 0.05$), while the value of OD_{260} in control group did not show any variation. With the treating time went by, the release of cell constituents increased. It was reported that the releasing of cell materials absorbed at 260 nm led to disruption of the cytoplasmic membrane properties²⁸. Soluble protein leakage of mycelium cell was shown in Fig. 3c. Soluble

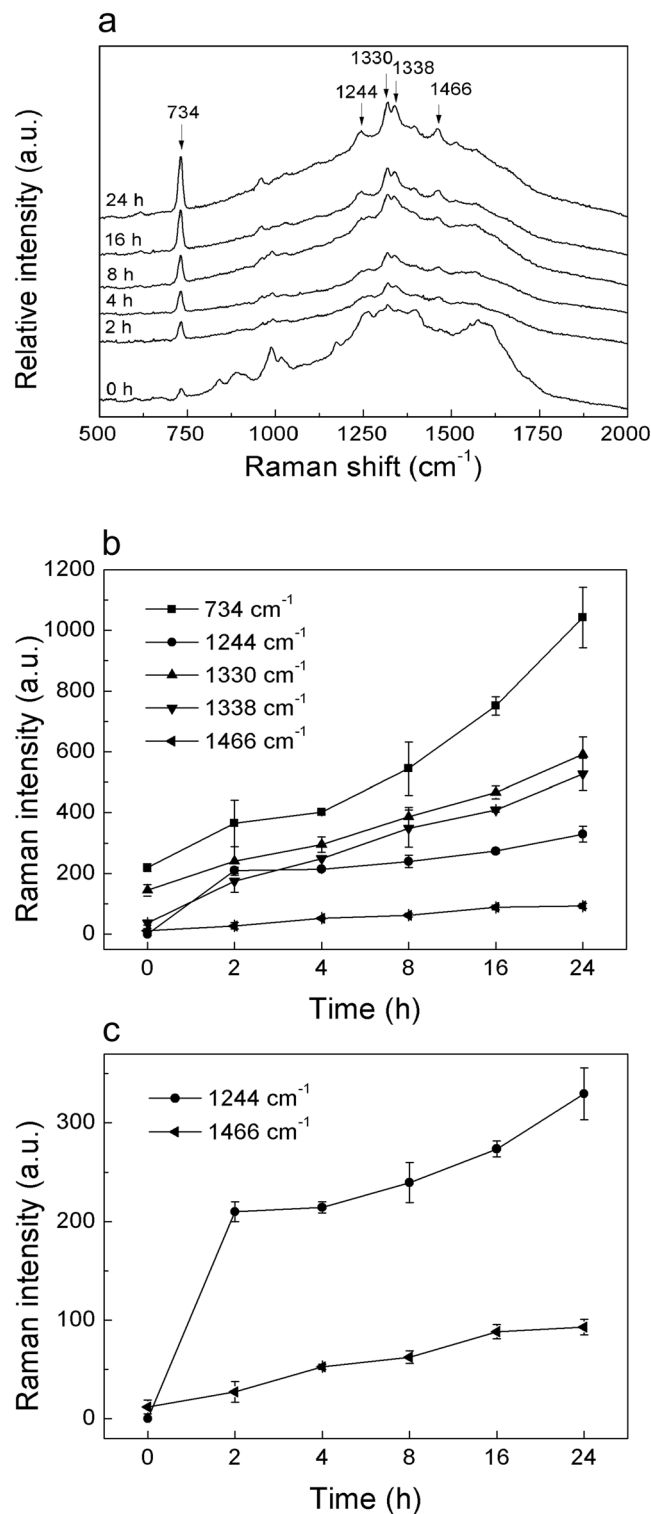


Figure 6. SERS spectra and extracted dataset. (a) SERS spectra of extracellular material after treatment with 2 MIC trans-cinnamaldehyde. (b) Trend of peak intensity at different Raman shift. (c) Magnified curve of Raman intensity at 1244 cm^{-1} and 1466 cm^{-1} .

protein in suspension increased with the incubation time in all group, but the test groups increased more drastically. The present study of constituents absorbing at 260 nm and soluble protein leaking from cells confirmed that trans-cinnamaldehyde disrupted the cytoplasmic membrane of *P. italicum*, and then led to cell death.

Efflux of potassium ions. Potassium ions efflux involved in permeability barrier of cytoplasmic membrane²⁹. However, maintaining ion homeostasis is integral to the maintenance of the energy status of the cell as

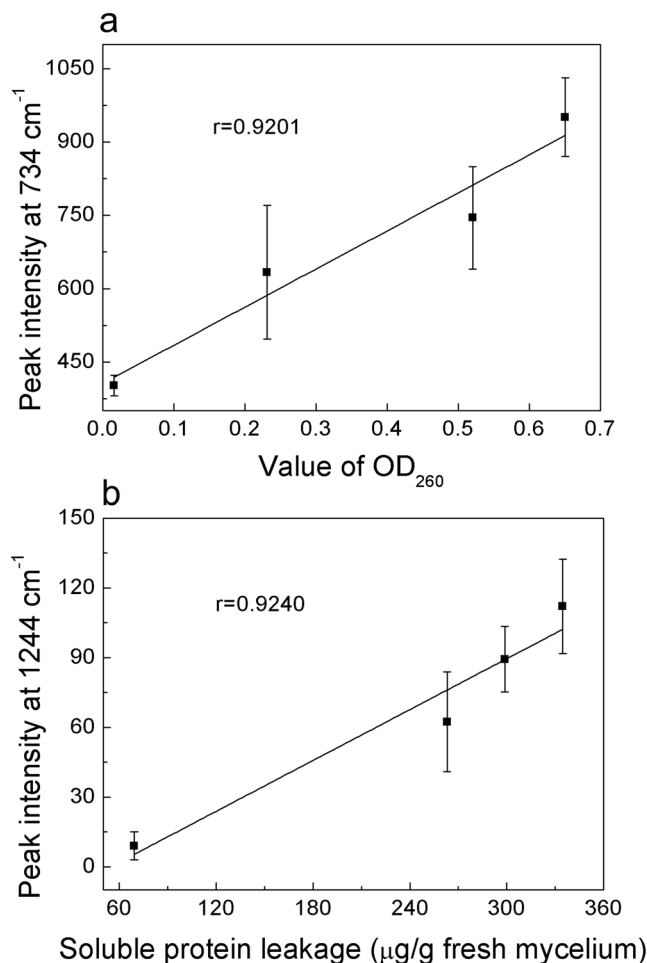


Figure 7. Correlation between Raman intensity and index from previous study. **(a)** The correlation curve between Raman intensity at 734 cm⁻¹ and OD₂₆₀ value after 2 h treatment of 2 MIC trans-cinnamaldehyde. **(b)** The correlation curve between Raman intensity at 1244 cm⁻¹ and soluble protein leakage after 2 h treatment of 2 MIC trans-cinnamaldehyde.

well as membrane-coupled, energy-dependent processes such as solute transport, regulation of metabolism, control of turgor pressure and motility³⁰. Even relatively slight changes to the structural integrity of cell membranes can detrimentally affect cell metabolism and lead to cell death²⁶. In this research, potassium ions efflux in test group were significantly higher than control group after 30 min treatment with trans-cinnamaldehyde ($P < 0.05$) as shown in Fig. 3d. High level of Potassium ions efflux indicated that trans-cinnamaldehyde severely damaged the plasma membrane of *P. italicum*.

Accumulation of reactive oxygen species. In order to assess whether the membrane of mitochondria has been damaged after trans-cinnamaldehyde treatment, level of ROS was determined. As shown in Fig. 4, level of ROS in 2 MIC treated group was significantly higher than other groups, which indicated that massive accumulation of ROS happened. It is widely accepted that massive ROS affects mitochondrial function such as oxidative phosphorylation and mitochondrial membrane permeability. In this case, trans-cinnamaldehyde treatment triggered the production of ROS and thus it accumulated, being a direct danger to mitochondria membrane.

Ultrastructure change of mycelium after treatment. SEM is a strong approach to study the ultrastructure of cells. The images of mycelium after various concentration of trans-cinnamaldehyde treatment had been presented in Fig. 5. The control (Fig. 5a) and low concentration group (Fig. 5b) showed a smooth appearance and straight body. It is obvious that the surface of mycelium had been sunken in Fig. 5c,d (group treated with 1 MIC and 2 MIC, respectively). Moreover, the group treated with 2 MIC presented a worse status where the surface was not only sunken but also distorted, suggesting that the structure of cell wall had been disordered so that the skeleton cannot support the cell.

SERS study on extracellular material. SERS provided ultrasensitive and fingerprint information of extracellular material after *P. italicum* treated with trans-cinnamaldehyde. Several typical strong SERS peaks were observed as shown in Fig. 6. Intensity at 734, 1330, 1338 cm⁻¹ were assigned to nucleic acid. And Intensity

at 1244 cm^{-1} was assigned to protein. In addition, intensity at 1466 cm^{-1} was assigned to lipid. According to Fig. 6a, the Raman intensity at 734 cm^{-1} increased dramatically along with the incubation time. Simultaneously, the Raman intensity at 1244 , 1330 , 1338 and 1466 cm^{-1} went up slowly relative to the baseline. All the detail trend of Raman intensity were elaborated in Fig. 6b,c, expressed as the intensity of individual peak.

Intensity at 734 cm^{-1} was found in adenine, adenosine or adenosine monophosphate (AMP) in previous study^{17,31}, which mean 734 cm^{-1} band was assigned to adenine. Further, it comes from adenine breathing mode³¹, precisely. The increase of the intensity at 734 cm^{-1} indicated that the concentration of adenine, adenosine or AMP in suspension raised, which mean that the permeability of plasma membrane had been changed, intracellular material like adenine, adenosine or AMP were able to go through the phospholipid bilayer. This result showed a strong correlation with the OD_{260} value which represented the nucleic acid, with a correlation coefficient of 0.9201 as shown in Fig. 7a. In addition, 1330 and 1338 cm^{-1} were assigned to nucleic acids³², the increase of their intensity indicated that the DNA or RNA had gone through the plasma membrane. Moreover, in SERS spectra of DNA, the 734 cm^{-1} band appears stronger for an open double strand due to better contact between the bases and the colloidal gold or silver compared to native DNA³¹. The appearance of the sharp and strong adenine ring breathing peak, after treated with trans-cinnamaldehyde, therefore indicates denaturation of the DNA of *P. italicum*.

Intensity at 1244 cm^{-1} was assigned to Amide-III of protein according to previous study^{32,33}. Peak at 1244 cm^{-1} went up gradually after 4 h treatment of trans-cinnamaldehyde as shown in Fig. 6a, which means the ascent of concentration of soluble protein in suspension. Here, it was similar to the soluble protein leakage test, implying that the plasma membrane was disordered. This result was intensively relative to the soluble protein leakage, with a correlation coefficient of 0.9240 shown in Fig. 7b.

Intensity at 1466 cm^{-1} was from lipid^{32,34}. Lipid is the main constituent of phospholipid bilayer, keeping the integrity of cell membrane so as to serve important functions in maintaining fungal viability²⁵. The increase of intensity at 1466 cm^{-1} in suspension indicated that trans-cinnamaldehyde destroyed the phospholipid bilayer of mycelium of *P. italicum*, finally, led to cell death.

Conclusion

To learn the mechanism of trans-cinnamaldehyde inhibiting *P. italicum*, to control the diseases of blue mold of citrus fruits and prevent economic losses. In this paper, we revealed the mechanism of trans-cinnamaldehyde inhibiting *P. italicum*, via membrane damage using SERS which offered ultrasensitive and fingerprint information. Membrane integrity test, Potassium ions efflux and membrane permeability tests indicated that the plasma membrane of *P. italicum* had been severely destroyed by trans-cinnamaldehyde and the cell wall collapsed referring to SEM images. Determination of ROS implied that mitochondria membrane would be disordered. SERS of supernatant suggested several Raman intensity increased, furthermore, peaks at 734 , 1330 and 1338 cm^{-1} were related to nuclei acid release, peak at 1244 cm^{-1} was related to protein leakage, and peak at 1466 cm^{-1} was related to lipid losses. The Raman intensity has shown a strong correlation with either OD_{260} value or soluble protein leakage, which mean SERS would be an alternative to analyze the antifungal mechanism of essential oil on fungus. All proves pointed to the damage of plasma membrane of *P. italicum* caused by trans-cinnamaldehyde. The future study will focus on the application of SERS on *in situ* detection of antifungal mechanism in living fungus.

References

- Zhu, R. *et al.* Postharvest Control of Green Mold Decay of Citrus Fruit Using Combined Treatment with Sodium Bicarbonate and *Rhodospiridium paludigenum*. *J. Food & Bioprocess Technology* **6**, 2925–2930 (2013).
- Droby, S. *et al.* Role of citrus volatiles in host recognition, germination and growth of *Penicillium digitatum* and *Penicillium italicum*. *J. Postharvest Biology & Technology* **49**, 386–396 (2008).
- Sharma, R. R., Singh, D. & Singh, R. Biological control of postharvest diseases of fruits and vegetables by microbial antagonists: a review. *J. Biological Control* **50**, 205–221 (2009).
- Askarne, L. *et al.* Use of Moroccan medicinal plant extracts as botanical fungicide against citrus blue mould. *J. Letters in Applied Microbiology* **56**, 37–43 (2013).
- Taguchi, Y. *et al.* The effect of cinnamaldehyde on the growth and the morphology of *Candida albicans*. *J. Medical Molecular Morphology* **46**, 8–13 (2013).
- Brasil, I. M. *et al.* Polysaccharide-based multilayered antimicrobial edible coating enhances quality of fresh-cut papaya. *J. LWT - Food Science and Technology* **47**, 39–45 (2012).
- Wu, Y. *et al.* Cinnamaldehyde inhibits the mycelial growth of *Geotrichum citri-aurantii* and induces defense responses against sour rot in citrus fruit. *J. Postharvest Biology & Technology* **129**, 23–28 (2017).
- Schuster, K. C. *et al.* Multidimensional information on the chemical composition of single bacterial cells by confocal Raman microspectroscopy. *J. Anal. Chem.* **72**, 5529–5534 (2000).
- Matthaus, C. *et al.* Noninvasive Imaging of Intracellular Lipid Metabolism in Macrophages by Raman Microscopy in Combination with Stable Isotopic Labeling. *J. Anal. Chem.* **84**, 8549–8556 (2012).
- Móricz, Á. M. *et al.* Raman spectroscopic evaluation of the influence of *Pseudomonas* bacteria on aflatoxin B1 in the BioArena complex bioautographic system. *J. Journal of Raman Spectroscopy* **39**, 1332–1337 (2010).
- Jarvis, R. M. & Goodacre, R. Discrimination of bacteria using surface-enhanced Raman spectroscopy. *J. Anal. Chem.* **76**, 40–47 (2004).
- Cui, L. *et al.* Sensitive and Versatile Detection of the Fouling Process and Fouling Propensity of Proteins on Polyvinylidene Fluoride Membranes via Surface-Enhanced Raman Spectroscopy. *J. Anal. Chem.* **83**, 1709–1716 (2011).
- Nanda, S.S., Yi, D.K. & Kim, K. Study of antibacterial mechanism of graphene oxide using Raman spectroscopy. *J. Sci Rep* **6**, 28443 (2016).
- Lu, X. *et al.* Infrared and Raman spectroscopic studies of the antimicrobial effects of garlic concentrates and diallyl constituents on foodborne pathogens. *J. Analytical Chemistry* **83**, 4137 (2011).
- Tao, Y. *et al.* Metabolic-activity based assessment of antimicrobial effects by D2O-labeled Single-Cell Raman Microspectroscopy. *J. Analytical Chemistry* **89**, 4108 (2017).
- Torkabadi, H. H. *et al.* Following Drug Uptake and Reactions inside *Escherichia coli* Cells by Raman Microspectroscopy. *J. Biochemistry* **53**, 4113–4121 (2014).
- Cui, L. *et al.* *In situ* study of the antibacterial activity and mechanism of action of silver nanoparticles by surface-enhanced Raman spectroscopy. *J. Analytical Chemistry* **85**, 5436–5443 (2013).

18. Bhowmick, T. K. *et al.* A study of the effect of JB particles on *Saccharomyces cerevisiae* (yeast) cells by Raman spectroscopy. *J. Journal of Raman Spectroscopy* **39**, 1859–1868 (2008).
19. Sujith, A. *et al.* Surface enhanced Raman scattering analyses of individual silver nanoaggregates on living single yeast cell wall. *J. Applied Physics Letters* **92** (2008).
20. Syamala, K. M. *et al.* Inhibition Assay of Yeast Cell Walls by Plasmon Resonance Rayleigh Scattering and Surface-Enhanced Raman Scattering Imaging. *J. Langmuir* **28**, 8952–8958 (2012).
21. Gerez, C. L. *et al.* Control of spoilage fungi by lactic acid bacteria. *J. Biological Control* **64**, 231–237 (2013).
22. Helal, G. A. *et al.* Effects of *Cymbopogon citratus* L. essential oil on the growth, lipid content and morphogenesis of *Aspergillus niger* ML2-strain. *J. Journal of Basic Microbiology* **46**, 456–469 (2006).
23. Liu, J. *et al.* Effects of chitosan on control of postharvest diseases and physiological responses of tomato fruit. *J. Postharvest Biology and Technology* **44**, 300–306 (2007).
24. da Rocha Neto, A. C., Maraschin, M. & Di Piero, R. M. Antifungal activity of salicylic acid against *Penicillium expansum* and its possible mechanisms of action. *J. International journal of food microbiology* **215**, 64–70 (2015).
25. Paul, S. *et al.* *Trachyspermum ammi* (L.) fruit essential oil influencing on membrane permeability and surface characteristics in inhibiting food-borne pathogens. *J. Food Control* **22**, 725–731 (2011).
26. Bajpai, V. K., Sharma, A. & Baek, K.-H. Antibacterial mode of action of *Cudrania tricuspidata* fruit essential oil, affecting membrane permeability and surface characteristics of food-borne pathogens. *J. Food Control* **32**, 582–590 (2013).
27. Helander, I. M. *et al.* Characterization of the action of selected essential oil components on gram-negative bacteria. *J. Journal of Agricultural & Food Chemistry* **46**, 3590–3595 (1998).
28. Oonmetta-Aree, J. *et al.* Antimicrobial properties and action of galangal (*Alpinia galanga* Linn.) on *Staphylococcus aureus*. *J. LWT - Food Science and Technology* **39**, 1214–1220 (2006).
29. Lambert, R. J. W. *et al.* A study of the minimum inhibitory concentration and mode of action of oregano essential oil, thymol and carvacrol. *J. Journal of applied microbiology* **91**, 453–462 (2001).
30. Sean, D. *et al.* Determining the Antimicrobial Actions of Tea Tree Oil. *J. Molecules* **6**, 87–91 (2001).
31. Haka, A. S. *et al.* Surface-Enhanced Raman Spectroscopy in Single Living Cells Using Gold Nanoparticles. *J. Applied Spectroscopy* **56**, 150–154 (2002).
32. Schuster, K. C., Urlaub, E. & Gapes, J. R. Single-cell analysis of bacteria by Raman microscopy: spectral information on the chemical composition of cells and on the heterogeneity in a culture. *Journal of Microbiological Methods* **42**, 29 (2000).
33. Tian, H. *et al.* Arsenic interception by cell wall of bacteria observed with surface-enhanced Raman scattering. *J. J Microbiol Methods* **89**, 153–158 (2012).
34. Maquelin, K. *et al.* Identification of medically relevant microorganisms by vibrational spectroscopy. *J. Journal of Microbiological Methods* **51**, 255–271 (2002).

Acknowledgements

The work described in this article was supported by National Key Technology R & D Program in the 13th Five Year Plan of China (2018YFC160015), the Natural Science Foundation of Jiangsu Province (BK20171139), Yangtze River Delta Project of Shanghai (18395810200), Forestry science and technology innovation and extension project of Jiangsu Province (No. LYKJ [2017] 26), National first-class discipline program of Food Science and Technology (JUFSTR20180509), Science and technology project of Jiangsu Bureau of Quality and Technical Supervision (KJ175923 and KJ185646), and Science and Technology Plan of Changzhou City (CE20172002).

Author Contributions

Fei Huang, Jie Kong and Jian Ju wrote the main manuscript text. Ying Zhang, Yahui Guo and Yuliang Cheng prepared figures 1–4. He Qian, Yunfei Xie prepared figures 5–7. Weirong Yao contributed the original idea to this paper that SERS can be used to study the antifungal mechanism.

Additional Information

Competing Interests: The authors declare no competing interests.

Publisher's note: Springer Nature remains neutral with regard to jurisdictional claims in published maps and institutional affiliations.



Open Access This article is licensed under a Creative Commons Attribution 4.0 International License, which permits use, sharing, adaptation, distribution and reproduction in any medium or format, as long as you give appropriate credit to the original author(s) and the source, provide a link to the Creative Commons license, and indicate if changes were made. The images or other third party material in this article are included in the article's Creative Commons license, unless indicated otherwise in a credit line to the material. If material is not included in the article's Creative Commons license and your intended use is not permitted by statutory regulation or exceeds the permitted use, you will need to obtain permission directly from the copyright holder. To view a copy of this license, visit <http://creativecommons.org/licenses/by/4.0/>.

© The Author(s) 2019